Properties of polyisobutylene polyurethane block copolymers: 2. Macroglycols produced by the 'inifer' technique

T. A. Speckhard, P. E. Gibson and S. L. Cooper*
Department of Chemical Engineering, University of Wisconsin, Madison, WI 53706, USA

and V. S. C. Chang and J. P. Kennedy
Institute of Polymer Science, The University of Akron, Akron, OH 44325
(Received 6 February 1984; revised 5 April 1984)

The structure–property relationships of a series of 4,4'-diphenylmethane diisocyanate (MDI) based polyisobutylene (PIB) polyurethanes were investigated. The PIB glycol was synthesized via the 'inifer' technique and had a narrow functionality distribution with a number average functionality of 2.0. The use of a PIB glycol with improved functionality and solution polymerization of the polyurethane led to improved mechanical properties compared with previously studied PIB polyurethanes. However, the mechanical properties were still low compared with conventional polyurethanes; the absence of soft segment strain-induced crystallization and compositional heterogeneity due to reactant incompatibility are cited as possible causes of low mechanical properties. Sample compositions were designed for independent investigation of the effects of hard segment content and soft segment molecular weight on the properties of the materials. Increasing hard segment content resulted in improved dynamic and tensile modulus, lower elongation at break, and larger hard segment domains. Increasing soft segment molecular weight led to larger domains and reduced mechanical properties. The degree of phase separation as measured by the soft segment T_g and the amount of interfacial mixing measured by small angle X-ray scattering (SAXS) were unaffected by hard segment content and soft segment molecular weight and were indicative of a high degree of phase separation compared with conventional polyurethanes.

(Keywords: polyisobutylene polyurethanes; block polymers; inifer; structure–property relationships; phase separation; small-angle X-ray scattering)

INTRODUCTION

Thermoplastic polyurethane elastomers are linear block copolymers of the $(AB)_n$ type. One block of the polymer is typically a polyether or polyester diol with a molecular weight 500–5000. These blocks are termed the soft segments because at the service temperature they exist in a rubbery or viscous state. In contrast, the so-called hard segments are, at the service temperature, in a glassy or semi-crystalline state. These segments are generally composed of aromatic diisocyanates chain extended with low molecular weight diols to produce blocks of molecular weight in the range of 500–3000. Dimensional stability is provided through microphase separation of the hard segments into domains which then act as a reinforcing filler and multifunctional crosslinks. The materials are thermoplastic because heating the hard segments above their glass transition or melting point will allow the material to flow. A wide range of physical properties and morphologies has been observed depending on the composition and chemical structure of the hard and soft segments[1–9].

The driving force for phase separation in these systems is the incompatibility of the two segment types. Generally, the urethane segments are more polar than the polyether or polyester segments. The driving force for phase separation is further increased by the ability of the urethane segments to form interurethane hydrogen bonds. Other factors influencing the phase separation of these materials include segment length, crystallizability of either segment, potential for soft segment–hard segment hydrogen bonding, sample composition, sample preparation, and mechanical and thermal history. Experimental evidence has shown that these materials are not completely phase separated but exhibit some degree of phase mixing[1–9]. It is thus more accurate to attempt to define the degree of phase separation compared to an ideally (completely) phase separated material.

Recently, polyurethanes based on hydrocarbon soft segments, primarily polybutadiene and polyisobutylene, have been investigated[7–27]. These materials are of interest for two major reasons. Compared to polyether or polyester polyurethanes, polyalkyl polyurethanes demonstrate superior hydrolytic stability and lower moisture permeability[7,9–11,21]. These materials are also of interest for the study of structure–property relationships in segmented polyurethanes[7,8,12–20]. Polyalkyl soft segments have no potential for hydrogen bonding and are less polar than the more conventional polyether or polyester soft segments. Thus, polyalkyl polyurethanes tend to be more completely phase separated than conventional polyurethanes[7,15–17,20].

Despite the increased degree of phase separation which is generally thought to improve mechanical properties[28], a review of the literature indicates that the mechanical

* Author to whom correspondence should be addressed.

0032-3861/85/010055-15$03.00
© 1985 Butterworth & Co. (Publishers) Ltd.

properties of polyalkyl polyurethanes are inferior compared to those of polyether or polyester polyurethanes. For example, for polybutadiene polyurethanes[12,16,17,26,27] the best reported tensile properties are tensile strengths of 10–20 MPa (1000 psi = 7 MPa) with elongations at break of 200–600%, while typical commercial polyether or polyester polyurethanes[28] possess tensile strengths of 30–60 MPa with elongations at break of 300–1000%. Explanations for the lower tensile properties of the polybutadiene polyurethanes have been concerned with the lack of the potential for soft segment crystallization under strain, incompatibility during polymerization producing macrophase separated materials, and the molecular weight and functionality of the hydroxy-terminated polybutadiene. Ono *et al.*[26] and Petrov and Lykin[27] studied the effect of polybutadiene molecular weight (number average) on material properties. Ono *et al.*[26] found that many properties improved as polybutadiene molecular weight decreased from 3000–1350, including a doubling of tensile strength from 5–10 MPa. This could be a significant factor since most of the reported work including the studies reporting optimum properties cited above has been done using polybutadiene soft segments with molecular weights greater than 2000. However, it should be noted that the materials studied by Ono *et al.* were prepared at a constant molar ratio of hard segment to soft segment. Thus, while the soft segment molecular weight decreased from 3000–1350 the hard segment content increased from approximately 25–70%. This large change in hard segment content casts doubt upon the attempt to interpret the variation in properties solely in terms of an effect of soft segment molecular weight. It should also be noted that the increase in tensile strength was accompanied by a decrease in elongation at break (600–200%). This tradeoff behaviour between tensile strength and elongation at break is customary with changes in hard segment content. Similar conclusions were reached by Petrov and Lykin[27] and Zapp *et al.*[24] on polybutadiene and polyisobutylene polyurethanes respectively. In both of these studies hard segment content varied inversely with soft segment molecular weight.

Problems associated with the functionality of the hydroxy terminated polybutadiene and its effects on mechanical properties have been studied by Petrov and Lykin[27] and Schneider *et al.*[15–17]. Petrov and Lykin studied materials based on soft segment polyols with functionalities less than two and found, as expected, that the mechanical properties improved as the average functionality of the polyol approached two. It is interesting to note that in the range of functionalities studied (1.65–1.98), the tensile strength tripled while the elongation at break only increased slightly. Similar results have been obtained on polyisobutylene polyurethanes[24]. Schneider *et al.* first[15,16] studied materials based on a hydroxy-terminated polybutadiene that had an average functionality greater than two with a broad distribution of functionalities. They suggested that the properties of the material suffered from some gel formation because of functionalities greater than 2 being present, network defects, and possibly low molecular weight because of the presence of the monofunctional oligomer fraction. In a later study[17], the polybutadiene macroglycol used had a narrow distribution of functionality with an average functionality of 1.97. However, there was not a dramatic improvement in tensile properties. Compared to their previous work the authors observed lower values of tensile strength and higher values of elongation at break, a result that might be expected on the basis of fewer crosslinks in the material. It should be noted that the polybutadiene used in the latter study had a high vinyl content which would be expected to inhibit strain-induced crystallization thus possibly reducing tensile properties.

Although the relative importance of strain-induced crystallization as a factor influencing tensile properties is not well established because of the many factors influencing mechanical properties[29] and the variety of parameters studied in the urethane literature, it is likely that the greater tensile strength and extensibility of conventional polyurethanes can at least be partially attributed to the fact that many of these materials are based on soft segments that can crystallize under strain. That is, polyalkyl based materials may have properties more comparable with polyester or polyether based materials in which the soft segments do not crystallize under strain. This conclusion is supported by data on typical polypropylene oxide based polyurethanes which are well known to possess somewhat lower tensile properties than polyurethanes made with crystallizable polyol components[30]. Also, Brunette *et al.*[16] studied the effect of hydrogenation of polybutadiene diols on the properties of polybutadiene polyurethanes. The authors noted that hydrogenation of polybutadiene would be expected to improve its crystallizability (the existence of *cis* and *trans* isomers due to the double bond would be eliminated) and they attributed their observed increase in tensile properties on hydrogenation to an increased effect of soft segment strain induced crystallization.

Polyisobutylene homopolymers and ionomers are known to exhibit soft segment crystallization under strain[31,32], however, no evidence of such behaviour was observed in a previous study of polyisobutylene polyurethanes[7]. The absence of this phenomenon is probably due to the restrictions placed on the PIB chain by the hard segment domains. It is also possible that insufficient strains were reached for crystallization to occur[32] or that the crystals melt below room temperature[31].

Reactant incompatibility during synthesis is another possible source of reduced mechanical properties. Most of the reported synthesis of polyalkyl polyurethanes has been done in bulk because the large polarity difference of the reactants makes finding a common solvent difficult. However, Xu *et al.*[8] have suggested that bulk polymerization of polybutadiene polyurethanes suffers from macrophase separation of the reaction components during the reaction resulting in compositional heterogeneity and less than optimum properties.

Xu's polybutadiene polyurethane material was found to be a blend of two segmented copolymers with very different average hard segment contents and average hard segment lengths. Similar results have been obtained for some polyether–polyester segmented copolymers[33]. Xu *et al.* have suggested that the phenomenon should be common in segmented copolymers, although it should be specially evident in systems with highly incompatible segments[8].

Most of the work discussed above has been done on polybutadiene based polyurethanes. Recently, we have

begun a study of polyisobutylene based polyurethanes[7]. Polyisobutylene offers two advantages over polybutadiene; it has superior oxidative stability[7,21] and structure–property studies are not complicated by the effects of isomeric content. It has also been suggested that polyisobutylene polyurethanes have potential biomedical applications[22]. In a previous study from this laboratory[7], the polyisobutylene prepolymer was produced via ozonolysis of an isobutylene–isoprene copolymer which resulted in a polyisobutylene glycol with a number average functionality (f_n) of 1.9, a number average molecular weight of 1430, and a polydispersity (M_w/M_n) of 1.9. The bulk synthesis of the corresponding polyurethanes suffered not only from the low functionality of the polyisobutylene glycol which limited the number average polyurethane molecular weight to about 10000 but also from incompatibility effects. These effects in turn led to rather poor mechanical properties.

In this contribution the study of the structure–property relationships of polyisobutylene polyurethanes has been extended to include materials based on polyisobutylene glycols produced by the 'inifer' technique[34,35]. The polyisobutylene glycol produced by this technique is hydroxy-terminated with a narrow functionality distribution and a f_n of 2.0[34,35]. The polyol also has a relatively narrow molecular weight distribution ($M_w/M_n = 1.5$)[35]. Thus the use of these materials should eliminate the functionality related problems of the previous study. Furthermore, in this study the polyurethane synthesis was carried out in solution with the expectation of reducing macroscale synthesis related incompatibility effects. Finally, several series of samples based on different soft segment molecular weights and hard segment contents were prepared that allow for separate investigation of the effects of these variables on the properties of the system. Note however that increasing either of these variables while holding the other constant causes an increase in the average hard segment length.

EXPERIMENTAL

Materials

The synthesis and purification of α,ω-di(hydroxy)polyisobutylene (PIB) has been described elsewhere[34,35]. 4,4′-Diphenylmethane diisocyanate (MDI) (Mobay) was vacuum distilled and stored under dry nitrogen before use. 1,4-Butanediol (BD) (Fisher Scientific) was distilled over molecular sieves (3Å) under dry nitrogen and stored over molecular sieves (3Å). Xylene and *N,N*-dimethylformamide (DMF) (Fisher Scientific) were refluxed under dry nitrogen over calcium hydride and freshly distilled into amber bottles before use[36].

Synthesis of polyisobutylene polyurethane

α,ω-di(hydroxy)polyisobutylene was dissolved in a mixture of dry DMF/xylene (25/75) under dry nitrogen atmosphere in a stainless steel enclosure, to make a 20% (w/v) solution at 75°C in a beaker over a hot plate[37]. A stoichiometrically calculated amount of MDI was added to the solution and stirred constantly with a glass rod for 1 h, then the appropriate amount of BD was added to the mixture with a microsyringe. The final ratio of OH/NCO was 1.0. After stirring for an additional hour, the mixture was poured onto an open Teflon pan and allowed to cure at 75°C for two days while the solvent was slowly evaporated. Subsequently the polyurethane film was placed in a vacuum oven at 85°–90°C for two days under vacuum before testing. The resulting films were approximately 0.3 to 0.6 mm thick. The materials synthesized are summarized in *Table 1*. The sample nomenclature, for example 4000–4/3/1, indicates a polyisobutylene number average molecular weight (4000) and a molar ratio (4:3:1) of MDI to BD to PIB.

Characterization methods

Differential scanning calorimetry (d.s.c.) thermograms were recorded from −110–230°C using a Perkin–Elmer D.S.C. 2 equipped with a data processing unit. The heating rate was 20°C min^{-1} and the quenching rate was 320°C min^{-1}. The data processing unit allowed automatic subtraction of the background and normalization of the thermograms for sample weight.

Dynamic mechanical data were obtained using a computer controlled Rheovibron DDV-II. Data were taken from −100°C until sample failure at a test frequency of 110 Hz and a temperature rise rate of 2°C min^{-1}.

Room temperature uniaxial stress–strain and stress hysteresis data were taken on an Instron table model tensile testing device. The rate of strain based on the initial gauge length was constant at 7.9 or 5.7% min^{-1}. Samples were prepared using an ASTM D1708 standard die. Hysteresis measurements were made by loading and unloading the sample at a constant rate of 7.9 or 5.7% min^{-1}, and were cyclically carried out to increasing strain levels.

Wide-angle X-ray scattering experiments were performed using a Picker Model 3667 A diffractometer in the reflectance mode. Intensity was scanned as a function of scattering angle from 2–40°.

Small angle X-ray scattering experiments were performed using the following apparatus and procedures. X-rays were produced by a rotating anode X-ray generator operating at 40 kV accelerating potential and 50 mA emission current. After emission from the copper anode, the X-rays passed through a nickel filter so that the X-ray wavelength was predominantly 0.1542 nm (CuK_α). A

Table 1 Materials

Sample*	Wt% MDI	Wt% MDI/BD
1800–8/7/1	45.1	59.4
1800–6/5/1	40.0	52.0
1800–4/3/1	32.6	41.4
1800–3/2/1	27.5	34.1
1800–2/1/1	20.9	24.7
3400–10/9/1	37.3	49.3
3400–8/7/1	33.2	43.6
3400–6/5/1	28.0	36.4
3400–4/3/1	21.4	27.2
3400–3/2/1	17.3	21.5
3400–2/1/1	12.5	14.8
4000–10/9/1	34.2	45.3
4000–8/7/1	30.2	39.7
4000–6/5/1	25.2	32.8
4000–4/3/1	19.0	24.1
11000–10/9/1	17.5	23.1
11000–8/7/1	14.7	19.3
11000–6/5/1	11.6	15.1

* Nomenclature is as follows: 1800–8/7/1 indicates PIB molecular weight of 1800 and an 8/7/1 molar ratio of MDI/BD/PIB

modified Kratky compact SAXS camera was used to collimate the X-rays into a beam which was about 1.25 cm by 100 μm at the sample. The collimation optics, the sample holder, and the scattering path were evacuated to eliminate scattering by air. The sample-to-detector distance was approximately 0.6 m. Scattered X-rays were detected by a one-dimensional position-sensitive detector and associated electronics. The SAXS data were collected by a multi-channel analyser and transferred to a computer for subsequent processing. Corrections were made to the data to take into account the detector sensitivity, the detector dark current, parasitic scattering, and sample absorption. Relative intensity data were converted to absolute intensity data by using a Lupolen (polyethylene) standard[38]. In order to eliminate slit-length smearing effects, an experimentally measured slit-length weighting function was used to desmear the data by the iterative method of Lake[39]. The range of sample thicknesses was from about 0.4 mm–1.0 mm while values of the linear attenuation coefficients varied between about 0.4 mm^{-1} and 0.5 mm^{-1}.

RESULTS AND DISCUSSION

Thermal analysis

D.s.c. thermograms for the 1800 PIB molecular weight materials are shown in *Figure 1*. High temperature thermograms of the second heating (after-quenching) of samples 1800–4/3/1 and 1800–8/7/1 are shown in *Figure 2*. *Figure 3* displays the initial run and the run following quenching for the 8/7/1 molar ratio samples with 3400, 4000 and 11 000 PIB molecular weight. Similar thermograms (not shown) were observed for other samples in those series. The soft segment glass transition data are summarized in *Table 2a* for all of the materials, with hard segment thermal transitions summarized in *Table 2b* for the 1800 series materials.

In general for block copolymers the position of the soft segment glass transition is primarily affected by the amount of hard segments dispersed in the soft segment phase and is often used as a relative measure of the degree of phase separation. The breadth of the transition zone may also be used as a qualitative measure of the degree of phase separation; however, the transition zone breadth is affected to a large extent by segmental mixing in the interfacial zone between phases in addition to mixing in each phase. *Figures 1* and *3* and *Table 2a* show that the soft segment glass transition is well defined and unaffected by

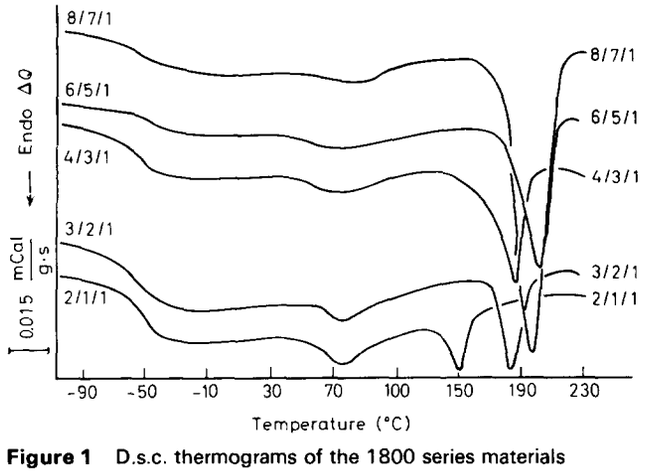

Figure 1 D.s.c. thermograms of the 1800 series materials

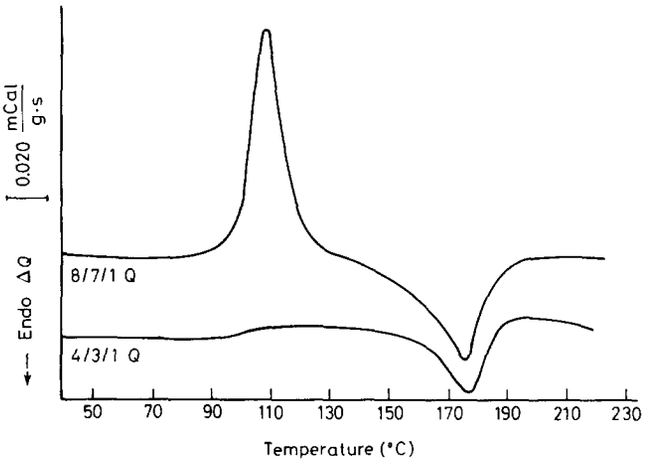

Figure 2 D.s.c. thermograms of the second heating following quenching for samples 1800-8/7/1 and 1800-4/3/1

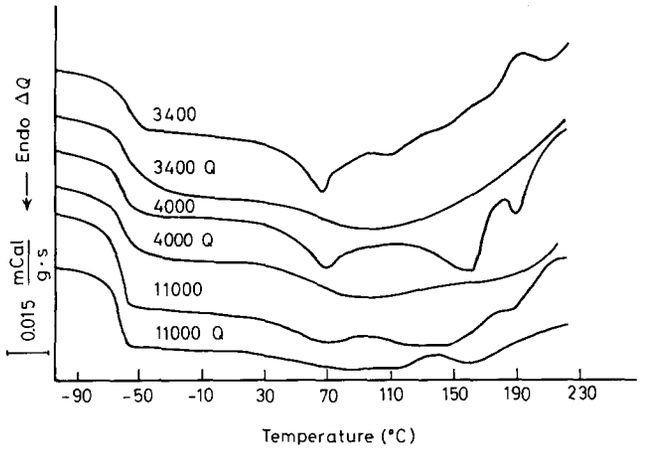

Figure 3 D.s.c. thermograms of the 8/7/1 series materials

heating and quenching. Also, except for sample 1800-8/7/1, there is no effect of hard segment content on the soft segment glass transition temperature. (Note that the soft segment glass transition was not well defined for sample 1800-8/7/1 (*Figure 1*) probably because of its low soft segment content. Thus the accuracy of the data in *Table 2a* for sample 1800-8/7/1 could be questioned.) The constancy of the soft segment glass transition is indicative of highly phase separated block copolymers; similar results have been seen in other polyalkyl polyurethanes[7,16,17]. Conventional polyurethanes often exhibit a large increase in the soft segment glass transition with increasing hard segment content which is attributed to an increase in the number of hard segments dispersed in the soft segment phase[40,41].

From *Table 2a* it can be seen that increasing PIB molecular weight results in a narrower glass transition centred at a lower temperature. Similar results have been reported previously for polyether and polyester polyurethanes[40–42]. Schneider and Paik Sung[40] attributed the decrease of the soft segment glass transition with increasing soft segment molecular weight to a decrease in phase mixing and hydrogen bonding. Critchfield *et al.*[41,42] noted that homopolymers generally exhibit a decrease in T_g with decreasing molecular weight that is interpreted as increased free volume associated with chain ends leading to increased mobility. They ascribed the

Table 2a Thermal transitions: Soft segment glass transition. (All values in °C)

Sample	d.s.c. First run T_g[a]	Breadth[b]	d.s.c. Quench run T_g[a]	Breadth[b]	Rheovibron (E''maximum) T_g
1800–8/7/1	–62	10	–62	10	–
6/5/1	–51	25	–52	25	–
4/3/1	–48	29	–50	28	–40
3/2/1	–48	29	–49	30	–39
2/1/1	–50	30	–50	30	–39
3400–10/9/1	–56	20	–57	20	–
8/7/1	–56	20	–57	21	–42
6/5/1	–57	21	–57	20	–44
4/3/1					–
3/2/1	–56	23	–58	19	–43
2/1/1					
4000–10/9/1	–61	15	–60	13	–43
8/7/1	–61	13	–60	12	–
6/5/1	–59	16	–60	17	–44
4/3/1	–58	15	–60	15	–44
11000–10/9/1	–61	11	–62	11	–48
8/7/1	–61	10	–62	10	–
6/5/1	–59	11	–62	11	–48

[a] D.s.c. T_g determined from midpoint of change in baseline height
[b] T_g breadth determined by intersections of baselines and tangent through midpoint

Table 2b Thermal transitions: Hard segment transitions

Sample	First run T_1 (°C)	T_M (°C)	ΔH_M	Quench run T_R (°C)	T_M (°C)	
1800–8/7/1	90	201	14.6	109	176	13.0
1800–6/5/1	66	204	9.2	121	180	8.8
1800–4/3/1	73	189	7.5	–	179	6.7
1800–3/2/1	76	187	5.0	–	179	2.5
1800–2/1/1	77	150	2.1	–	–	–

T_1 = position of low temperature disordering endotherm
Tm = position of high temperature hard segment melting or disordering endotherm
ΔHm = enthalpy of Tm endotherm (Joules/g)
T_R = position of hard segment crystallization or ordering exotherm
– = indicates no apparent transition

increase in T_g with decreasing molecular weight in segmented copolymers to decreases in free volume and mobility due to bonding of the soft segments to the rigid isocyanate blocks. Since their materials did not exhibit a significant shift in soft segment T_g with hard segment content they did not think that decreased phase mixing was an important factor. This conclusion could also be drawn from the data in *Table 2a*. It appears that the decrease in the breadth and position of the glass transition zone with increasing soft segment molecular weight is a result of decreasing influence of chain end restrictions and interfacial effects as the soft segment chain length increases.

The high temperature multiple endothermic behaviour exhibited on the initial scans shown in *Figure 3* is commonly observed in MDI/BD based polyurethanes and has been attributed to melting or disordering of ordered hard segment regions of different extent or degree of ordering[6,42,43]. Endotherms above about 190°C have been associated with melting of hard segment crystallites[40]. *Figure 3* also shows that endothermic behaviour is diminished on the quenched run, presumably because quenching was too fast for the ordered structures present in the initial run to reform.

From *Figure 1* it can be seen that the 1800 series materials display a distinct high temperature (150–210°C) endotherm (T_m) and a broad endotherm (T_1) between 50–100°C. Van Bogart *et al.*[43] attributed the broad, low temperature endotherm to a low degree of hard segment ordering resulting from storage (annealing) at room temperature. T_m is associated with the melting of hard segment crystallites. *Table 2* shows that ΔH_m increases with hard segment content as might be expected. A plot of ΔH_m *versus* hard segment content (*Figure 4*) is linear and extrapolates to $\Delta H_m = 0$ at a hard segment content of about 20% (MDI/BD). This could indicate that a roughly constant fraction of the hard segments are crystalline in the 1800 series materials and that more than one MDI/BD segment may be needed to form crystallites[42]. Wide angle X-ray diffraction (WAXD) revealed MDI/BD crystalline peaks[6] superimposed on an amorphous background for materials with a high hard segment content and long hard segment lengths such as sample 1800-8/7/1. Shorter hard segments probably form crystalline-like regions that are too small or disordered to be seen by WAXD.

Figure 2 shows high temperature thermograms of the quenched run for samples 1800-4/3/1 and 1800-8/7/1.

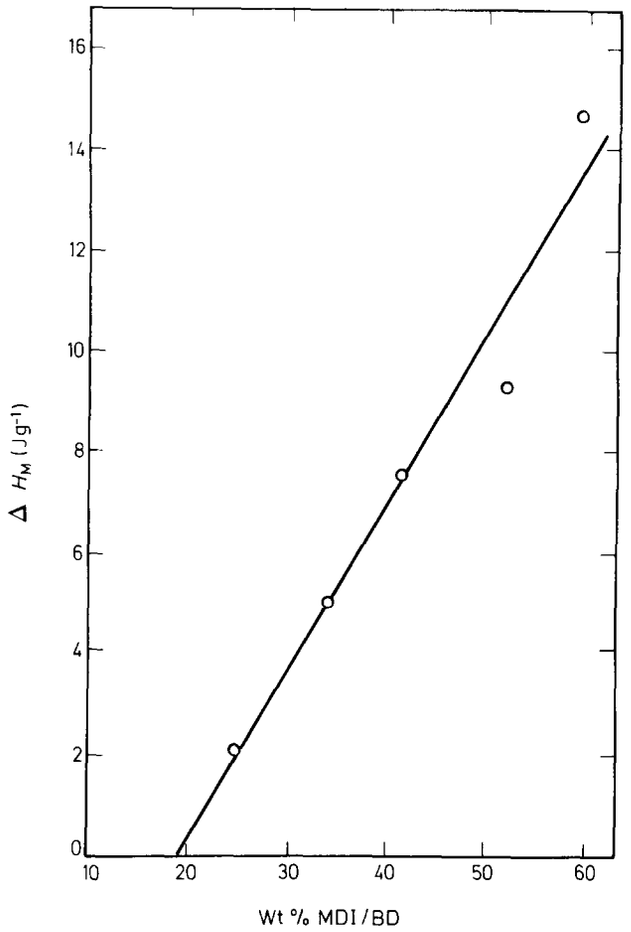

Figure 4 Enthalpy of hard segment disordering as a function of hard segment content for the 1800 series materials. (○): Data; (———): least squares fit

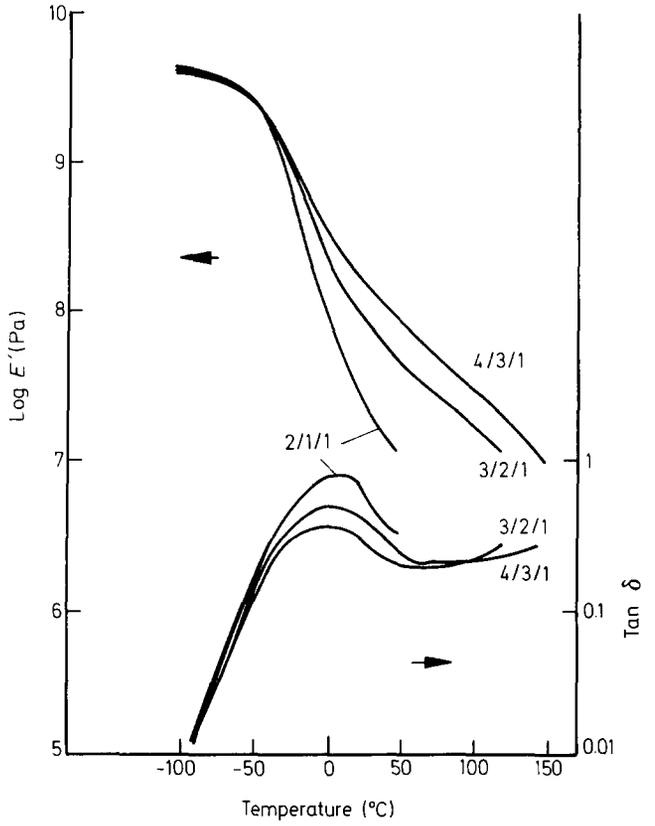

Figure 5 Storage modulus (E') and tan δ curves for the 1800 series materials

Samples 1800-8/7/1 and 1800-6/5/1 (not shown) displayed a distinct exotherm (T_R, *Table 2b*) at approximately 100–130°C. Similar behaviour has been reported previously for conventional and polybutadiene polyurethanes[44–46] and has been attributed to recrystallization or reordering processes of the hard segment units. Apparently in these materials recrystallization is fast enough that it can occur during heating in the d.s.c. Brunette and MacKnight[44] in their study on polybutadiene polyurethanes noted that recrystallization could be avoided by using a 160°C min^{-1} scan rate. Despite the occurrence of recrystallization, samples 1800-8/7/1 and 1800-6/5/1 exhibit subsequent melting endotherms that are quite similar to those displayed by samples 1800-4/3/1 and 1800-3/2/1 which do not possess distinct recrystallization exotherms. In all cases the endotherms on the quenched run are broader, smaller, and are centered at a lower temperature compared with the endotherms of the initial run demonstrating that quenching does diminish the degree of hard segment ordering.

Dynamic mechanical testing

The results of dynamic mechanical measurements are displayed in *Figures 5–8* and E'' peak position data are recorded in *Table 2a*. *Figures 5* and *6* show the results for the 1800 series samples (1800-6/5/1 and 1800-8/7/1 were too brittle for mechanical testing). *Table 2a* and *Figure 6* indicate that the glass transition temperature as measured by the position of the E'' peak does not vary with hard segment content in accord with the d.s.c. data. The fact

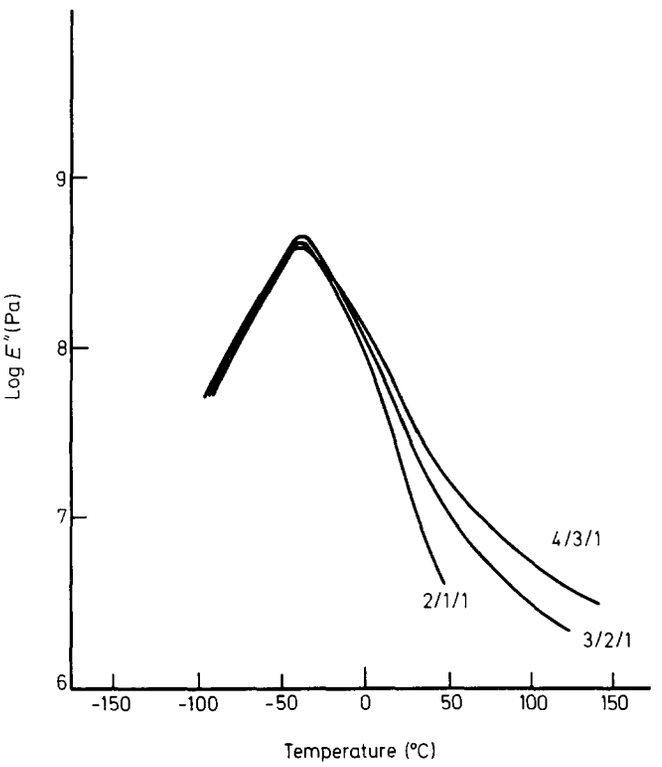

Figure 6 Loss modulus (E'') curves for the 1800 series materials

that the E'' peak is typically 10–15° higher than the glass transition temperature measured by d.s.c. is a result of the high frequency (110 Hz) of the dynamic mechanical test[42].

The 1800 series materials also exhibit the expected increase in the storage modulus (*Figure 5*) above the soft

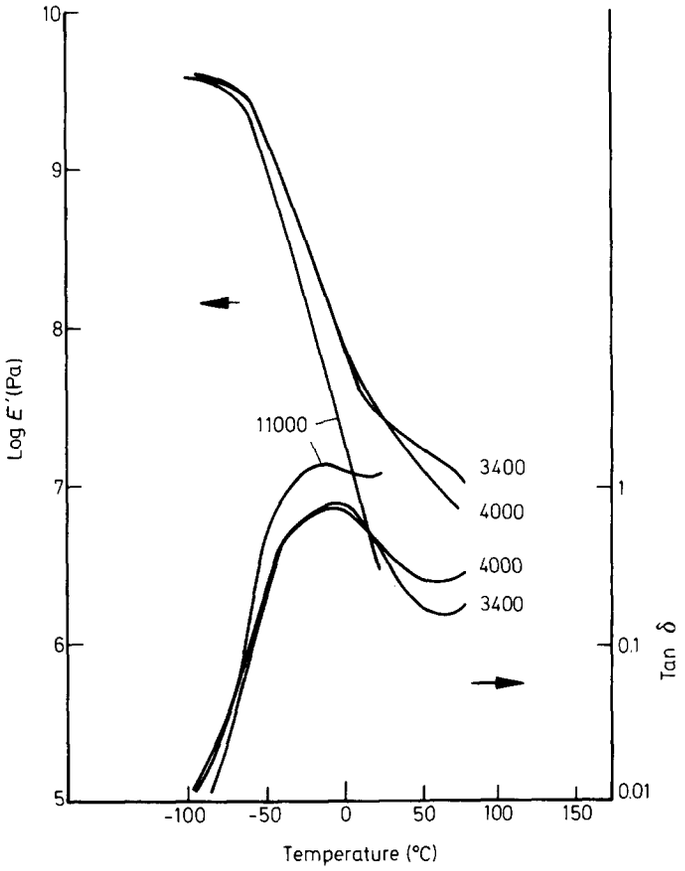

Figure 7 Storage modulus (E') and tan δ curves for the 6/5/1 series materials

phase glass transition with increasing hard segment content[1,7,17]. The 3400, 4000 and 11 000 series materials show the same trend. However, as noted previously for polyisobutylene polyurethanes[7], the storage modulus does not exhibit a well defined plateau region but tends to gradually decrease with increasing temperature above the soft phase glass transition. Previously[7], this behaviour was attributed to the low molecular weight of the overall polyurethane. Although the materials of this study exhibit plateaus extended to somewhat higher temperatures at equivalent hard segment contents that are roughly comparable to high temperature softening points observed for polybutadiene polyurethanes[17], the softening points are still low compared to conventional polyurethanes. Ryan[12] has suggested that low softening points may be an inherent feature of polyalkyl polyurethanes. The gradual drop off in modulus may be a result of heterogeneity in chemical composition. A polyurethane block copolymer in which the hard segment content varied widely from molecule to molecule would be expected to show a broad softening transition region. Nielsen[47] has shown that chemically heterogeneous copolymers exhibit very broad transition zones compared with copolymers that are homogeneous in composition.

The dynamic mechanical properties of samples 3400-6/5/1, 4000-6/5/1 and 11000-6/5/1 are shown in *Figures 7* and *8*. These samples exhibit properties that are typical of the other samples in each series. *Figure 7* and *Table 2a* show a slight decrease in soft segment T_g as measured by the position of the E'' peak with increasing soft segment molecular weight in agreement with the d.s.c. data. The storage modulus data (*Figure 7*) indicate that sample 11000-6/5/1 is probably a one phase material since there is not even a change in slope in the drop off of the curve above the soft phase glass transition. This would not be unexpected in view of the low hard segment content (12% MDI) of the sample. However, the d.s.c. data discussed above and the SAXS data to be presented later suggest that this sample is a two phase material. It may be that if the sample contains small, isolated hard segment domains they may have a negligible effect on the response of the long PIB segments due to the small applied strain in the dynamic mechanical test. *Figure 7* also shows that sample 3400-6/5/1 exhibits a slightly higher modulus above the soft phase glass transition compared with sample 4000-6/5/1 which is probably a result of its slightly higher hard segment content.

To determine the effect of soft segment molecular weight (or hard and soft segment block length) on the dynamic mechanical properties, samples of similar hard segment content should be compared. A careful examination of *Figures 4* and *6* reveals that sample 1800-3/2/1 which has a hard segment content between the hard segment contents of samples 3400-6/5/1 and 4000-6/5/1 has a greater storage modulus than either of those samples. Comparisons between other samples indicate a general trend of decreasing storage modulus with increasing soft segment molecular weight. The drop-off in modulus was most prominent between the 1800 and 3400 series samples. The hard segment crystallinity as measured by d.s.c. also shows a large decrease in going from the 1800 to the 3400 series samples indicating that hard segment crystallinity could be a factor leading to increased modulus. The effect of soft segment molecular weight on mechanical properties will be discussed further in the next section.

Tensile properties

Stress–strain curves for the 1800 series materials and samples 3400-8/7/1, 4000-8/7/1 and 11000-8/7/1 are

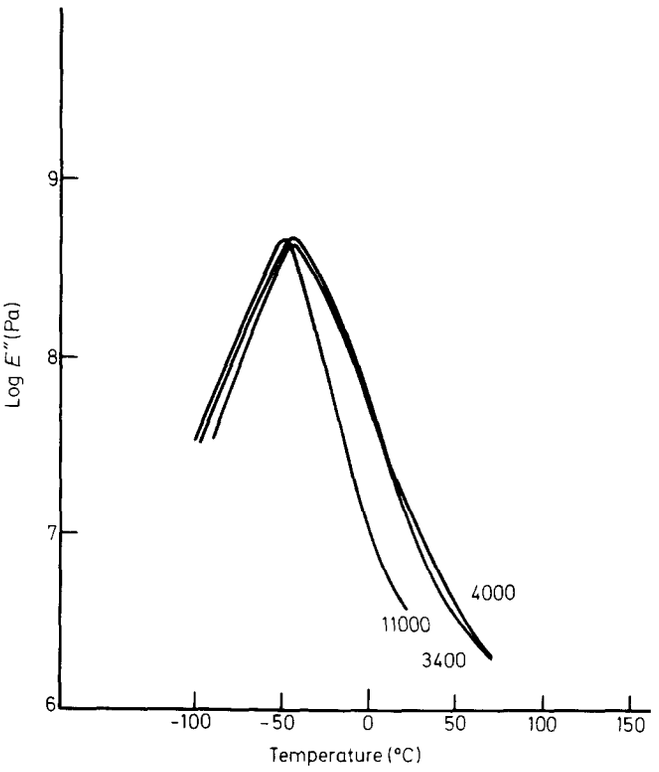

Figure 8 Loss modulus (E'') curves for the 6/5/1 series materials

shown in *Figure 9*. Results for all of the samples along with hysteresis values for the 3400, 4000 and 11000 series are summarized in *Table 3*. The most notable features of these data are the relatively low elongations (< 250% except for sample 3400-3/2/1) and tensile strengths (< 11 MPa) of the materials. As noted in the introduction, polyalkyl polyurethanes generally possess lower tensile properties than conventional polyurethanes. The various explanations for this behaviour discussed in the Introduction will be examined in light of the conclusions drawn from the data presented here.

The most dramatic difference between the data presented here and those reported previously[7] is the low value (10–30%) of hysteresis observed in this study compared with the 50–90% hysteresis noted previously. The high values reported were attributed to the low molecular weight of the polyurethane. Thus it appears that the materials studied in this investigation have a higher molecular weight. This conclusion is also supported by the more extended plateau region noted in the dynamic mechanical data and might be expected due to the better functionality of the polyisobutylene polyol. Another factor leading to low hysteresis values in the present study is the low hard segment content of the samples.

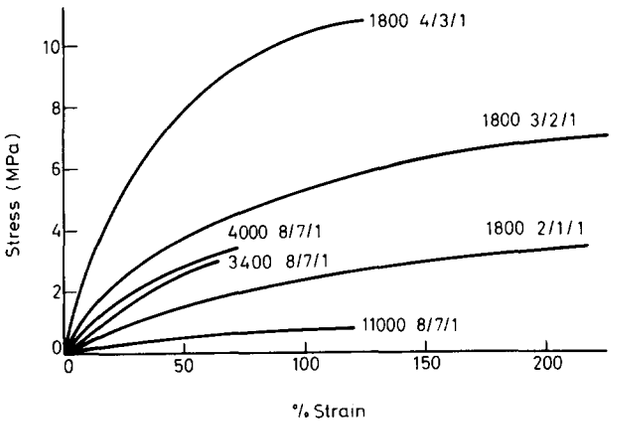

Figure 9 Stress-strain curves for the 1800 and 8/7/1 series materials

Increasing hard segment content also results in the usual tradeoff between increasing modulus and decreasing elongation at break[1,7,17,46]. One factor leading to low tensile strengths is that at high hard segment contents (> 45% MDI/BD) the materials become very brittle and break at very low elongations (< 20%). Conventional polyurethanes can exhibit elongations at break of almost 300% at 70% hard segment content[48]. This brittle behaviour may be a result of compositional heterogeneity; polybutadiene polyurethanes that exhibit brittle behaviour at high hard segment contents[17] have been shown[8] to be a blend of very low and very high hard segment content materials. Apparently, the properties of the high hard segment content fraction are dominant giving rise to properties that are similar to those of a brittle plastic.

The effect of soft segment molecular weight on tensile properties can be seen in *Figure 9*. Sample 1800-4/3/1 which possesses a hard segment content between the hard segment contents of samples 3400-8/7/1 and 4000-8/7/1 has a much greater modulus, tensile strength, and elongation at break. Comparisons with other samples reveals that increasing soft segment molecular weight generally results in lower mechanical properties consistent with the dynamic modulus data. Previous studies[24,26,27] on the effect of soft segment molecular weight on the properties of polyalkyl polyurethanes have indicated that optimum properties are obtained in the range of 1000–2000 number average molecular weight. However, as noted in the introduction, these studies did not keep the hard segment content constant. The hard segment content varied inversely with the soft segment molecular weight thereby making interpretation of the results solely in terms of the effect of soft segment molecular weight, difficult.

Several other studies of the effect of soft segment molecular weight on mechanical properties in conventional polyurethanes have also been complicated by variations in hard segment content[6,40,41,49]. Yet the

Table 3 Tensile properties

Sample	E_{100} (MPa)	σ_b (MPa)	ϵ_b%	% Hysteresis at 20% strain
1800–8/7/1	–	–	–	–
6/5/1	–	–	–	–
4/3/1	10.3	10.4	120	–
3/2/1	5.3	6.9	230	–
2/1/1	2.3	3.5	215	–
3400–10/5/1	–	1.7	15	–
8/7/1	–	3.0	65	20
6/5/1	–	4.4	70	20
4/3/1	1.4	1.9	155	25
3/2/1	1.3	5.6	615	10
2/1/1	0.6	1.1	215	15
4000–10/9/1	–	2.5	25	25
8/7/1	–	3.4	75	15
6/5/1	–	2.1	70	20
4/3/1	–	1.5	80	27
11000–10/5/1		0.73	95	20
8/7/1	0.64	0.7	110	20
6/5/1	0.67	1.2	175	15

E_{100} = secant modulus at 100% elongation
σ_b = engineering stress at break
ϵ_b = elongation at break

conclusions drawn from these studies are in basic agreement with those drawn from investigations[42,50] in which the soft segment molecular weight was varied at constant hard segment content. In most cases polyurethanes possessing soft segment molecular weights in the range of 2000–3000 were found to have optimum properties. Materials based on lower soft segment molecular weights suffered from a lower degree of phase separation and an inability of the soft segments to crystallize under strain. Smith[51] has suggested that smaller hard segment domains (at equivalent volume fractions) should be more effective at stopping catastrophic crack growth through the soft segment matrix. At equivalent hard segment contents, lower soft segment molecular weight materials have shorter average hard segment sequence lengths and might be expected to have smaller hard segment domains. Thus since polyalkyl polyurethanes do not demonstrate a marked improvement in either the degree of phase separation or the ability to crystallize under strain with increasing soft segment molecular weight, it is not surprising that optimum properties appear to be obtained for polyalkyl polyurethanes in a lower molecular weight range. The effect of domain size on tensile properties will be further examined on the basis of the SAXS results presented in the next section.

Of the possible explanations discussed in the introduction for the inferior mechanical properties of polyalkyl polyurethanes compared with conventional polyurethanes it appears that their inability to crystallize under strain and incompatibility effects leading to compositional heterogeneity during polymerization and possibly low overall molecular weight merit further study. We plan to investigate these effects in future work. Although soft segment molecular weight and functionality do influence mechanical properties it does not appear that optimizing these parameters will by itself produce properties comparable to those of conventional polyurethanes. Although polyisobutylene homopolymers and ionomers are known to exhibit soft segment crystallization under strain[31,32], no evidence of such behaviour was observed in this study. The absence of this phenomenon is probably due to the restrictions placed on the PIB chain by the hard segment domains. It is also possible that insufficient strains (except in the case of 3400-3/2/1) were reached for crystallization to occur[32] or that the crystals melt below room temperature[31]. The anomalous behaviour of sample 3400-3/2/1 could be related to strain-induced crystallization although the usual upturn in stress at high elongations was not observed. It would seem that in order to study the effect of soft segment crystallization under strain, either low temperature tensile experiments are necessary or soft segments other than polyisobutylene (hydrogenated polybutadiene[16] is one possibility) will have to be investigated.

Small angle X-ray scattering analysis

Small angle X-ray scattering curves for the 1800 and 4000 series samples are shown in *Figures 10* and *11*. Results for all of the samples are summarized in *Table 4*. In *Figures 10* and *11*, the absolute desmeared intensity normalized for the scattering from an electron (I_e) and the scattering volume (V) is plotted as a function of q, the magnitude of the momentum transfer vector. By definition, q is $\frac{4\pi}{\lambda}\sin\theta$ where λ is the wavelength of the X-rays and 2θ is the scattering angle. Before discussing the SAXS results given in *Table 4*, the method used to analyse the scattering curves is described. The analysis is based upon the assumption that the samples consist of two phases of different electron density. In the case of ideal phase separation, the two phases would be pure hard segment and pure soft segment so that a step change in electron density would exist at any phase boundary. The morphology-dependent parameters obtained by analysis

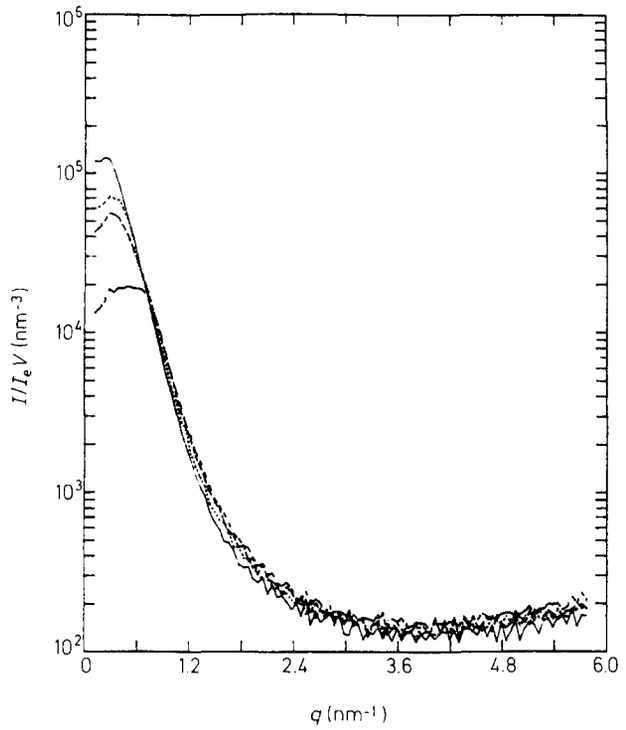

Figure 10 Desmeared and corrected SAXS curves for the 1800 series materials. (——) 10/9/1; (·····) 8/7/1; (-----) 6/5/1; (-·-·-) 4/3/1

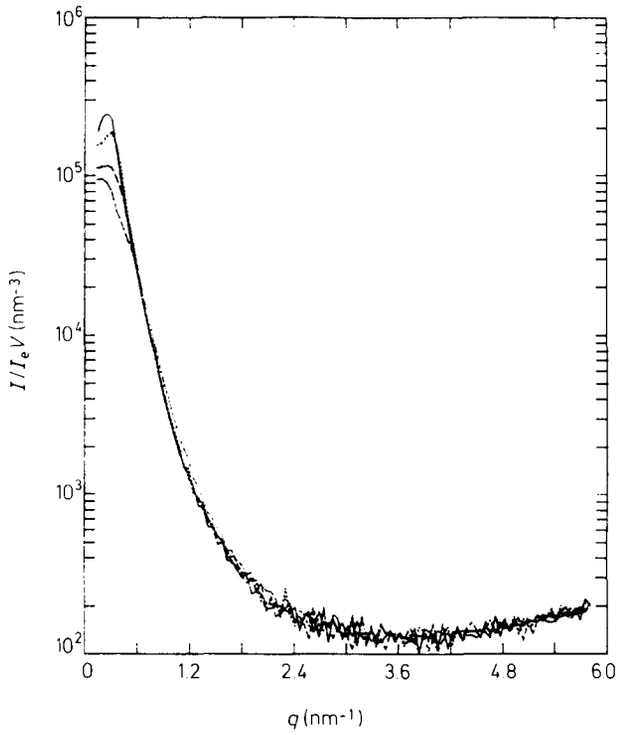

Figure 11 Desmeared and corrected SAXS curves for the 4000 series materials. (——) 6/5/1; (·····) 4/3/1; (-----) 3/2/1; (-·-·-) 2/1/1

Table 4 SAXS parameters

Sample	l_p nm	σ nm	$\overline{\Delta\rho^2}_{ideal}$*	$\overline{\Delta\rho^{2'}}$*	$\overline{\Delta\rho^{2''}}$*	$\frac{\overline{\Delta\rho^{2'}}^{a}}{\overline{\Delta\rho^2}_{ideal}}$	$\frac{\overline{\Delta\rho^{2'}}^{b}_{ideal}}{\overline{\Delta\rho^{2''}}} - 1$	$\frac{\overline{\Delta\rho^{2''}}^{c}}{\overline{\Delta\rho^{2'}}} - 1$
1800–6/5/1	4.1	0.4	4.70	1.56	2.08	0.33	1.3	0.33
4/3/1	3.7	0.3	4.28	1.45	1.70	0.34	1.5	0.18
3/2/1	3.4	0.2	3.80	1.45	1.67	0.38	1.3	0.15
2/1/1	2.4	0.3	2.98	1.13	1.46	0.38	1.0	0.29
3400–10/9/1	5.6	0.2	4.63	1.34	1.47	0.29	2.1	0.10
8/7/1	5.1	0.4	4.40	1.43	1.74	0.33	1.5	0.22
6/5/1	4.9	0	3.97	1.43	–	0.36	1.8	–
4/3/1	3.9	0.2	3.21	1.22	1.30	0.38	1.5	0.07
3/2/1	3.1	0.2	2.65	1.08	1.29	0.41	1.1	0.19
2/1/1	2.5	0.2	1.91	0.85	0.96	0.44	1.0	0.13
4000–10/9/1	5.6	0.6	4.48	1.39	2.26	0.31	1.0	0.62
8/7/1	5.3	0.3	4.18	1.42	1.61	0.34	1.6	0.13
6/5/1	4.7	0.2	3.70	1.21	1.32	0.33	1.8	0.09
4/3/1	3.8	0.2	2.92	1.12	1.26	0.38	1.3	0.12
11000–10/9/1	5.0	0.3	2.82	0.72	0.81	0.25	2.5	0.10
8/7/1	4.8	0.2	2.41	0.71	0.77	0.30	2.1	0.08
6/5/1	4.4	0.3	1.94	0.64	0.76	0.33	1.6	0.19

* (moles electrons $cm^{-3})^2 \times 10^3$
l_p = Porod's inhomogeneity length
σ = interfacial thickness parameter
$\overline{\Delta\rho^2}_{ideal}$ = calculated electron density variance assuming pure phases and sharp interfaces
$\overline{\Delta\rho^2}$ = experimental electron density variance excluding thermal density fluctuations
[a] a measure of the overall degree of phase separation
[b] a measure of the amount of segmental mixing in domains
[c] a measure of the amount of interfacial mixing
$\overline{\Delta\rho^2}$ = experimental electron density variance excluding thermal density fluctuations and diffuse interface effects

of the SAXS data included:

(1) an inhomogeneity length which characterizes the scale of the phase separation,

(2) an interfacial thickness parameter which gives a relative measure of breadth of the interface between domains, and

(3) three semiquantitative parameters describing the overall degree of phase separation, the extent of interfacial mixing, and the degree of phase mixing in domains.

Following Ruland[52], it is assumed that the absolute intensity, $I(q)$, can be written as the sum of contributions from SAXS, $I_s(q)$, and from background scattering, $I_b(q)$, due to density fluctuations within phases

$$I(q) = I_s(q) + I_b(q) \tag{1}$$

Several different expressions for approximating $I_b(q)$ have been proposed[53]. In this analysis both Ruland's expression[54]

$$I_b(q) = A\exp(bq^2) \tag{2}$$

and Vonk's expression[55]

$$I_b(q) = A + (bq)^{2m} \qquad \text{with } m = 1,2,3 \tag{3}$$

were examined. The results of fitting procedures to be subsequently described indicated that Vonk's expression with $m=2$ provided the best approximation of $I_b(q)$. For an ideal two phase system $I_s(q)$ is given by Porod's law[56]

$$\lim_{q\to\infty} I_s(q) = \frac{K}{q^4} \tag{4}$$

which must be modified in the case of a narrow interfacial zone between phases[52,57]

$$\lim_{q\to\infty} I_s(q) = \frac{KH^2(q)}{q^4} \tag{5}$$

Several expressions for $H^2(q)$ based on different models of the interfacial zone have been proposed[58]. In this analysis both a sigmoidal gradient where

$$H^2(q) = \exp(-\sigma^2 q^2) \tag{6}$$

and a Cahn–Hilliard[7,59,60] type of interface where

$$H^2(q) = \left[\frac{x}{\sinh(x)}\right]^2 \tag{7}$$

and $x = q\sigma\sqrt{3}$ were investigated.

In both cases σ is an interfacial thickness parameter related to the breadth of the interfacial region. In these models an ideal two-phase system has $\sigma = 0$ and $H^2(q) = 1$. The results of the fitting procedure described below indicated that slightly better fits to the data were obtained using the Cahn–Hilliard expression for $H^2(q)$.

For a two-phase material with sharp interfaces, the variance in electron density due to small angle X-ray scattering is given by

$$\overline{\Delta\rho^2} = \phi_h(\rho_h - \bar{\rho})^2 + \phi_s(\rho_s - \bar{\rho})^2 = \phi_h(1-\phi_h)(\rho_h - \rho_s)^2 \tag{8}$$

where ρ_h, ρ_s are the electron densities of the two phases (designated hard and soft here), ϕ_h, ϕ_s = volume fractions of the phases, and $\bar{\rho}$ = average electron density. For the case of no phase mixing (i.e. pure phases) $\overline{\Delta\rho^2}$ is identified

as $\overline{\Delta\rho^2}$ ideal. The experimental electron density variance is less than $\overline{\Delta\rho^2}_{ideal}$ as a result of phase mixing in domains and at the interface between domains.

The electron density variance due to SAXS can be determined from the relation[7]

$$\overline{\Delta\rho^2}' = \frac{1}{2\pi^2}\int_0^\infty q^2 I_s(q)\mathrm{d}q \tag{9}$$

Note that the effects of thermal density fluctuations $I_b(q)$ have been removed. The effects of diffuse interfaces on the electron density variance can be corrected for using the expression

$$\overline{\Delta\rho^2}'' = \frac{1}{2\pi^2}\int_0^\infty \frac{q^2 I_s(q)\mathrm{d}q}{H^2(q)} \tag{10}$$

The calculation of the integrals in equations (9) and (10) requires extrapolation of the low angle data to $q=0$ and the high angle data to $q\rightarrow\infty$. For the low angle extrapolation it was assumed that the function $G(q)=q^2I_s(q)$ approaches zero as q approaches zero. The high angle data was extrapolated by the following method. If there is some q^* such that Porod's law, as given by equation (5) holds for all $q \geqslant q^*$, then equation (9) can be rewritten as

$$\overline{\Delta\rho^2}' = \frac{1}{2\pi^2}\int_0^{q^*} q^2 I_s(q)\mathrm{d}q + \int_{q^*}^\infty \frac{K}{q^2}H^2(q)\mathrm{d}q \tag{11}$$

and equation 10 can be rewritten as

$$\overline{\Delta\rho^2}'' = \frac{1}{2\pi^2}\int_0^{q^*} \frac{q^2 I_s(q)\mathrm{d}q}{H^2(q)} + \frac{K}{q^*} \tag{12}$$

Neumuller and Bonart have noted that failing to extrapolate the high angle data and including its contribution to the integral can noticeably affect the calculation of the electron density variance[61]. The choice of q^* is arbitrary and does not influence the results[61]. In all cases q^* was set equal to 4.0 nm^{-1} and a cubic spline fitting procedure was used to determine $G(q)$ over the interval $q\varepsilon[0,q^*]$.

As shown originally by Bonart and Muller[62,63] and recently by Koberstein and Stein[57] and Van Bogart *et al.*[6], the comparison of these three variances ($\overline{\Delta\rho^2}_{ideal}$, $\overline{\Delta\rho^2}'$, $\overline{\Delta\rho^2}''$) provides information about the state and degree of phase separation. The degree of overall phase separation is reflected by the ratio

$$\overline{\Delta\rho^2}'/\overline{\Delta\rho^2}_{ideal} \tag{13}$$

which is one for the case of complete phase separation and decreases with increased phase mixing. The quantity

$$(\overline{\Delta\rho^2}_{ideal}/\overline{\Delta\rho^2}'') - 1 \tag{14}$$

is indicative of the amount of phase mixing within domains irrespective of the diffuseness of the interface. For the case of no phase mixing within domains its value is zero. The presence of interfacial mixing, irrespective of mixing within domains, is indicated by

$$\overline{\Delta\rho^2}''/\overline{\Delta\rho^2}' - 1 \tag{15}$$

which is zero for the case of sharp interfaces and increases with the breadth of the interface. The information obtained from these expressions is valuable in assessing the degree and origin (within domains or at the interface) of phase mixing. In order to calculate $\overline{\Delta\rho^2}_{ideal}$ accurate values of ρ_s and ρ_h are needed. Normally homopolymer values are used; however, in the case of MDI/BD, ρ_H is dependent on the degree of crystallinity. Furthermore, the existence of crystallinity in the MDI/BD phases as indicated by the d.s.c. results suggests that in actuality a three phase system is being studied. However, calculations indicate that for these samples the scattering due to the existence of both amorphous and crystalline MDI/BD phases is small compared to the scattering arising from the PIB and MDI/BD phases and so the samples were treated as psuedo two-phase systems. Values of 1.25[64] and 0.917[65] g cm^{-3} were used for the density of MDI/BD and PIB respectively in the calculation of $\overline{\Delta\rho^2}_{ideal}$. Although the absolute value of $\overline{\Delta\rho^2}_{ideal}$ is highly dependent on the density values used, the relative trends in $\overline{\Delta\rho^2}_{ideal}$ and associated parameters are not affected by the inaccuracies in ρ_h and ρ_s.

For a two-phase material with sharp interfaces, Porod showed that[55]

$$K = 2\pi(\rho_h - \rho_s)^2\left(\frac{S}{V}\right) \tag{16}$$

where S/V is the interfacial area per unit volume.

Combining expressions (8) and (16) yields

$$\left(\frac{S}{V}\right) = \frac{K}{2\pi}\frac{\phi_h(1-\phi_h)}{\overline{\Delta\rho^2}} \tag{17}$$

Porod's inhomogeneity length for a two-phase system with sharp interfaces is given by the relation[66]:

$$\frac{1}{l_p} = \frac{1}{4\phi_h(1-\phi_h)}\left(\frac{S}{V}\right) \tag{18}$$

Substitution of relation (17) in equation (18) allows calculation of Porod's inhomogeneity length without knowledge of the volume fractions:

$$l_p = \frac{8\pi\overline{\Delta\rho^2}}{K} \tag{19}$$

Since Porod's inhomogeneity length is only defined for systems with sharp interfaces, the appropriate electron density variance to use in equation (19) is $\overline{\Delta\rho^2}''$.[64]

After correcting, normalizing and desmearing the raw data, a non-linear regression was used to fit the scattering curves to the expression

$$I(q) = \frac{KH^2(q)}{q^4} + I_b(q) \tag{20}$$

substituting equations (2), (3), (6) and (7) for $I_b(q)$ and $H^2(q)$. Ruland[54] has derived a criterion for determining

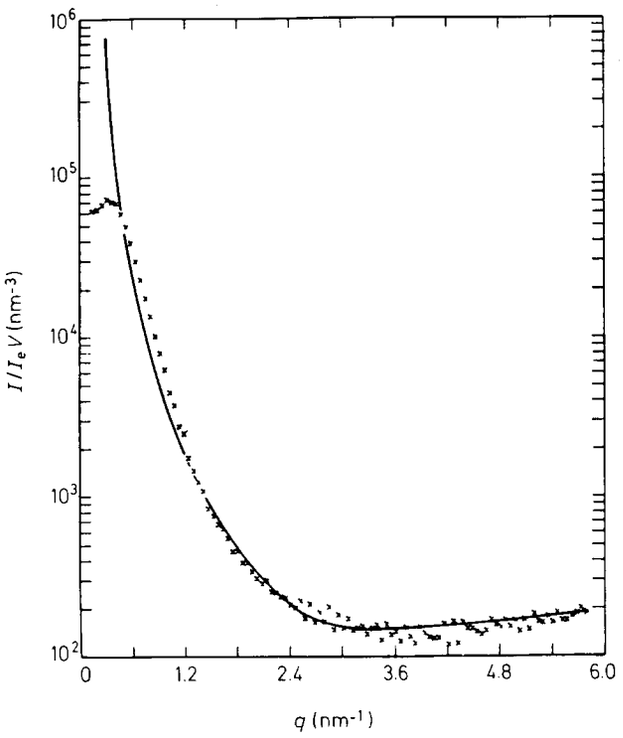

Figure 12 Experimental SAXS data and model fit for sample 1800-4/3/1. (×): data; (–) fit based on equation (20)

the minimum value of q at which Porod's law is valid. This criterion shows that Porod's law should hold at q values larger than the value corresponding to roughly the position of a secondary maximum in the scattering curve[57]. For each sample the q value corresponding to the maximum $q^2I(q)$ value (q at the peak) was determined and the lower limit of the fit range was arbitrarily fixed at 2.5 times q at the peak. This choice of q is somewhat conservative and as shown in the sample fits (*Figures 12* and *13*), and as noted previously[57], Porod's law often holds at lower q values. In general, the absolute values of the calculated SAXS parameters were slightly dependent on the minimum q value chosen for the fit range but consistent trends in the parameters were not dependent on the choice of fit range.

Initially, all four parameters, K, σ, A and b, were determined by fitting the data using equation (20) over the range 2.5 times q at the peak to $q = 5.7$ nm^{-1} (high angle limit of data). However, it was found that better fits to the data could be obtained by first fitting the expression for $I_b(q)$ to the data in the region of $q = 4.5$–5.7 nm^{-1}. In this region the contribution to the total scattering of $I_s(q)$ is negligible. The values of A and b determined in this manner were fixed and then values of K and σ were determined by fitting equation (20) from 2.5 times q at the peak to $q = 5.7$ nm^{-1}. For all samples it was found that Vonk's expression (equation (3)) gave the best fit to $I_b(q)$ while the Cahn–Hilliard expression (equation (7)) for $H^2(q)$ gave the best fits for $I_s(q)$. Fits obtained using this procedure are shown in *Figure 12* for sample 1800-4/3/1 (q peak $\times 2.5 = 1.33$ nm^{-1}) and *Figure 13* for sample 4000-8/7/1 (q peak $\times 2.5 = 0.93$ nm^{-1}). In both cases the fit is quite good over the desired fit range. The fit for sample 1800-4/3/1 shows a noticeable deviation from the data at lower q values while the fit for 4000-8/7/1 appears to hold at lower q values than $2.5 \times q$ peak indicating that Porod's law may be valid in that range. Generally fits to the 3400, 4000 and 11 000 series samples were satisfactory at lower q values than $2.5 \times q$ peak while the 1800 series fits showed significant deviations at lower q values.

SAXS results

The SAXS data shown in *Figures 10* and *11* and the parameters listed in *Table 4* exhibit distinct trends with hard segment content and soft segment molecular weight. *Figures 9* and *10* show a decrease in peak height and a slight shift of the peak to higher angles with decreasing hard segment content. The differences are not as pronounced in the 4000 series (*Figure 11*) because the change in hard segment content from sample to sample is not as great. In accord with the movement of the peak to higher angles, the long or interdomain spacings calculated from the peak of a plot of $q^2I(q)$ *versus* q decreased with decreasing hard segment content. (Interdomain spacings ranged from 8–20 nm.) A decreasing interdomain spacing is associated with decreasing domain size. This trend is also reflected in a decreasing inhomogeneity length as shown in *Table 4*. Calculating the individual hard and soft phase inhomogeneity lengths (using volume fractions calculated by assuming complete phase separation) reveals that the hard phase inhomogeneity length decreases while the soft phase inhomogeneity length increases with decreasing hard segment content. These trends would be expected since in this case hard segment content is proportional to average hard segment sequence length; similar results have been observed for polyisobutylene[7] and polyester polyurethanes[6].

The trend of decreasing peak height with decreasing hard segment content noted in *Figures 10* and *11* is usually reflected in lower values of the electron density variance $\overline{\Delta\rho^2}$ as shown in *Table 4*. However, because of the q^2 weighting factor in the calculation of $\overline{\Delta\rho^2}$ small differences in $I(q)$ at large angles can sometimes compensate for larger differences at smaller angles. *Table 4*

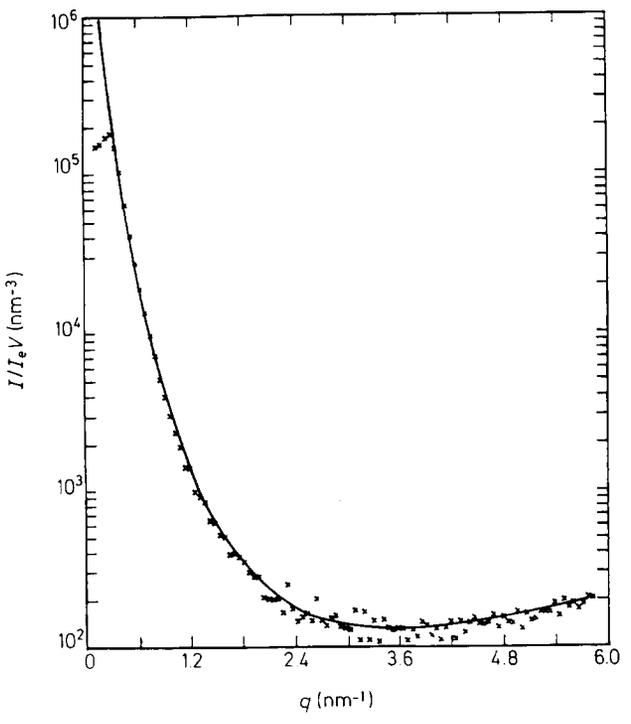

Figure 13 Experimental SAXS data and model fit for sample 4000-8/7/1. (×): data; (–) fit based on equation (20)

also shows that $\overline{\Delta\rho^2}_{ideal}$ decreases with decreasing hard segment content. This dropoff is due to a decrease in the $\phi_h(1-\phi_h)$ term (equation (8)) since ϕ_h is always less than 0.5 and decreases with decreasing hard segment content. In fact, the dropoff of $\overline{\Delta\rho^2}_{ideal}$ with decreasing hard segment content is faster than that of $\overline{\Delta\rho^{2\prime}}$ which is reflected in an increasing degree of phase separation as measured by $\overline{\Delta\rho^{2\prime}}/\overline{\Delta\rho^2}_{ideal}$ (*Table 4*). An increasing degree of phase separation with decreasing hard segment content has been suggested for conventional polyurethanes[6,7,40,41] and is attributed to a decrease in the number of hard segments dispersed in the soft phase. This conclusion is based on a decreasing soft segment T_g with decreasing hard segment content[6,7,40,41]; however, a similar trend was not observed with these samples. Bonart and Muller[63] have suggested that for conventional polyurethanes there are more soft segments included in the hard segment domains than hard segments dissolved in the soft segment phase. Thus, it could be that the apparent increased phase mixing with increasing hard segment content is occurring primarily in the hard segment domains or in the interfacial region. Phase mixing in the interfacial region as measured by the interfacial thickness σ or $\overline{\Delta\rho^{2\prime\prime}}/\overline{\Delta\rho^{2\prime}}-1$ however shows no clear trend with hard segment content. The extent of phase mixing in domains as measured by $\overline{\Delta\rho^2}_{ideal}/\overline{\Delta\rho^{2\prime\prime}}-1$ does generally increase with increasing hard segment content. Since there do not seem to be differences in phase mixing with changes in hard segment content in the soft phase due to the constancy of the soft segment T_g, or the interfacial region, the only apparent alternative is to postulate increased phase mixing in the hard segment domains with increasing hard segment content.

The effect of soft segment molecular weight on the various SAXS parameters can be discerned by comparing samples of approximately equal hard segment content. Interfacial thickness (σ) and the degree of interfacial mixing $\overline{\Delta\rho^{2\prime\prime}}/\overline{\Delta\rho^{2\prime}}-1$ do not exhibit a general trend with soft segment molecular weight. However, the overall degree of phase mixing ($\overline{\Delta\rho^{2\prime}}/\overline{\Delta\rho^2}_{ideal}$) and the extent of phase mixing in domains ($\overline{\Delta\rho^2}_{ideal}/\overline{\Delta\rho^{2\prime\prime}}-1$) show a slight trend towards increased mixing with increasing soft segment molecular weight (or hard and soft segment sequence lengths). This trend is in opposition to thermodynamic arguments[67] and experimental data on conventional polyurethanes[6,7]; however, it could partially explain the decrease in mechanical properties with increasing block lengths. One possible explanation for the observed trend is that longer hard segments are less mobile and may not be able to pack as easily, leading to incorporation of soft segments into the hard segment domain. This argument could also be used to explain the effect of hard segment content on phase separation since hard segment content and hard segment block length are not independent variables. It should also be noted that both increasing hard segment content and soft segment molecular weight lead to increased hard segment domain size which may facilitate the incorporation of the soft segments into the hard segment domains. Obviously, additional X-ray studies are needed to see if these trends are generally characteristic of polyurethane block copolymers.

Table 4 also shows that the inhomogeneity length increases with increasing soft segment molecular weight at similar hard segment contents. That is, domain size increases with block length as might be expected. This trend also supports the suggestion that the higher tensile properties of the shorter block length materials are due to their smaller domain sizes or greater interfacial areas (note the reciprocal relationships of l_p and S/V in equation (18)). As noted by Smith[51], smaller hard segment domains at equivalent volume fractions should more effectively stop catastrophic crack growth through the soft segment matrix. The SAXS data do not suggest an explanation for the superior tensile properties of sample 3400-3/2/1 other than its relatively high degree of phase separation.

Comparing the results presented here to other polyurethane systems is difficult because of the large effect of sample composition, structure and preparation method on the SAXS data; the variety of methods used to analyse SAXS data; and the lack of published data on many systems such as the polybutadiene polyurethanes. The values of the inhomogeneity length and long spacing obtained in this analysis are comparable to values for other polyurethanes in the literature[6,7,57]. It is interesting to note that the polyisobutylene polyurethanes studied previously[7] have shorter block lengths than the materials studied here and have generally smaller inhomogeneity lengths. As noted above, the effects of hard segment content on domain size and the degree of phase separation have been observed previously[6]. The absolute values of the degree of phase separation, $\overline{\Delta\rho^{2\prime}}/\overline{\Delta\rho^2}_{ideal}$, and the extent of mixing in domains, $\overline{\Delta\rho^2}_{ideal}/\overline{\Delta\rho^2}-1$, are highly dependent on the values for the phase densities used to calculate $\overline{\Delta\rho^2}_{ideal}$ thus making the possibility of direct comparisons difficult. Direct comparison with other MDI based polyether[57] and polyester[6] polyurethanes indicates that the degree of phase separation for the polyisobutylene polyurethanes is roughly the same while the degree of mixing in domains is greater for these polyisobutylene polyurethanes. A parameter which does not require density values for its calculation is the degree of interfacial mixing, $\overline{\Delta\rho^{2\prime\prime}}/\overline{\Delta\rho^{2\prime}}-1$. In this case, conventional MDI based polyurethanes[6,57] exhibit values for the degree of interfacial mixing of 0.5–0.8 and interfacial thicknesses (based on a sigmoidal gradient) of 0.7–1.0 nm. Thus the polyisobutylene polyurethanes of this study have less interfacial mixing than conventional polyurethanes which would support the assertion that polyalkyl based polyurethanes have a higher degree of phase separation than conventional polyurethanes.

SUMMARY

The structure–property relationships of a series of MDI based polyisobutylene polyurethanes were investigated using d.s.c., dynamic mechanical analysis, SAXS, and stress–strain and stress–hysteresis testing. The PIB glycol used was synthesized by the 'inifer' technique leading to a narrow functionality distribution and an average functionality of 2.0. The improved functionality of the PIB glycol and solution polymerization of the polyurethane block copolymer were utilized to overcome synthesis problems of an earlier study that led to low molecular weight materials and poor mechanical properties. Dynamic mechanical and tensile data indicated a slight improvement in mechanical properties compared with the materials studied previously, yet the properties were still low compared with conventional polyurethanes. The inability

of the soft segments to crystallize under strain and compositional heterogeneity due to reactant incompatability were suggested as possible causes for the low mechanical properties.

Hard segment content and soft segment molecular weight (or hard and soft segment block length) were the major factors influencing material properties. Unlike many other studies in the literature, the sample compositions were designed for independent investigation of these effects. The soft segment glass transition as measured by d.s.c. and dynamic mechanical spectroscopy was unaffected by hard segment content, indicative of a high degree of phase separation. There was a slight decrease in the soft segment T_g with increasing soft segment molecular weight attributed to a decreasing influence of chain-end restrictions and interfacial effects as the soft segment chain length increased. The dynamic mechanical and tensile modulus increased with increasing hard segment content while the elongation at break decreased. The existence of compositional heterogeneity was suggested by the brittle behaviour of high hard segment content materials and the gradual decrease of the dynamic mechanical modulus above the soft segment T_g. Increasing block length led to much poorer tensile properties attributed to a smaller hard segment domain interfacial area which should be less effective at stopping catastrophic crack growth through the soft segment matrix.

SAXS results showed an increase in domain size (smaller interfacial area) with increasing soft segment molecular weight. Increasing hard segment content resulted in larger hard segment domains and an apparent lower degree of phase separation. Increasing soft segment molecular weight also led to an apparent lower degree of phase separation in opposition to thermodynamic theory. Both effects could be due to difficulties in packing long hard segments into hard segment domains. The extent of interfacial mixing did not vary with hard segment content or soft segment molecular weight and was much lower than the degree of interfacial mixing observed for conventional polyurethanes, indicating a higher degree of phase separation in polyisobutylene polyurethanes.

ACKNOWLEDGEMENTS

The authors would like to thank J. Y. Chien for his help with the tensile experiments. Three of the authors (T.A.S., P.E.G and S.L.C.) would like to acknowledge partial support of this research by the Office of Naval Research and the Naval Air Systems Command. Two of the authors (V.S.C.C. and J.P.K.) would like to acknowledge partial support of this work by the National Science Foundation under grant DMR-81-20964).

REFERENCES

1 Estes, G. M., Cooper, S. L. and Tobolsky, A. V. *J. Macromol. Sci., Rev. Macromol. Chem.* 1970, **4**, 313
2 Cooper, S. L. and Estes, G. M., Eds., 'Multiphase Polymers', Adv. Chem. Ser. 176, American Chemical Society, Washington, D.C., USA, 1979
3 Schneider, N. S., Desper, C. R., Illinger, J. L. and King, A. O. *J. Macromol. Sci.-Phys.* 1975, **B11**, 527
4 Gibson, P. E., Vallance, M. A. and Cooper, S. L. in 'Properties of Polyurethane Block Polymers', Developments in Block Copolymers, (Ed. I. Goodman), Elsevier, Applied Sci. Publ., London, 1982
5 Van Bogart, J. W. C., Lilaonitkul, A., Lerner, L. and Cooper, S. L. *J. Macromol Sci.-Phys.* 1970, **B17**, 267
6 Van Bogart, J. W. C., Gibson, P. E. and Cooper, S. L. *J. Polym. Sci.-Polym. Phys.* 1983, **21**, 65
7 Speckhard, T. A., Ver Strate, G., Gibson, P. E. and Cooper, S. L. *Polym. Eng. Sci.* 1983, **23**, 337
8 Xu, M., MacKnight, W. J., Chen, C. H. Y. and Thomas, E. L. *Polymer* 1983, **24**, 1327
9 Arnold, Jr. C. *J. Elast. Plast.* 1974, **6**, 238
10 Gahimer, F. H. and Nieske, F. W. *Insulation (Libertyville, Ill)*, 39, Aug. 1968
11 Houghton, R. M. and Williamson, D. A. *SPE J.* 1971, **27**, 43
12 Ryan, P. W. *Brit. Polym. J.* 1971, **3**, 145
13 Ryan, P. W. *J. Elastoplast.* 1971, **3**, 57
14 Ryan, P. W. *Rubber World* 1971, **163**, 47
15 Schneider, N. S. and Matton, W. *Polym. Eng. Sci.* 1979, **19**, 1122
16 Brunette, C. M., Hsu, S. L., MacKnight, W. J. and Schneider, N. S. *Polym. Eng. Sci.* 1981, **21**, 163
17 Brunette, C. M., Hsu, S. L., Rossman, M., MacKnight, W. J. and Schneider, N. S. *Polym. Eng. Sci.* 1981, **21**, 668
18 Dequatre, C., Camberlin, Y., Pillot, L. and Pascault, J. P. *Angew. Macromol. Chem.* 1978, **72**, 11
19 Camberlin, Y., Gole, J., Pascault, J. P., Durand, J. P. and Dawans, F. *Macromol. Chem.* 1979, **180**, 2309
20 Camberlin, Y., Pascault, J. P., Letoffe, M. and Claudy, P. *J. Polym. Sci.* 1982, **20**, 1445
21 Chang, V. S. C. and Kennedy, J. P. *Polym. Bull.* 1983, **8**, 69
22 Giusti, P., Palua, M., Artigiani, F. and Soldani, G. IUPAC Prepr., p. 371, July 1982
23 Consaga, J. P. *J. Appl. Polym. Sci.* 1970, **14**, 2157
24 Zapp, R. L., Serniuk, G. E. and Minckler, L. S. *Rubber Chem. Technol.* 1970, **43**, 1154
25 Ivan, B. and Kennedy, J. P. *Am. Chem. Soc., Div. Org. Coat. Plast. Prepr.* 1980, **43**, 909
26 Ono, K., Shimada, H., Nishimura, T., Yamashita, S., Okamoto, H. and Minoura, Y. *J. Appl. Polym. Sci.* 1977, **21**, 3323
27 Petrov, G. N. and Lykin, A. S. *Polym. Sci. USSR*, 1979, **20**, 1351
28 Lilaonitkul A. and Cooper, S. L. 'Advances in Urethane Science and Technology', Vol. 7, p. 163 (Eds. K. C. Frisch and S. L. Reegan), Technomic Publ. Co., 1979
29 Smith, T. L. *J. Polym. Sci.-Polym. Phys. Edn.* 1974, **12**, 1825
30 Shibatani, K., Lyman, D. J., Shieh, D. R. and Knutson, K. *J. Polym. Sci., Polym. Chem. Edn.* 1977, **15**, 1665
31 Kato, M. and Mark, J. E. *Rubber Chem. Technol.* 1976, **49**, 85
32 Bagrodia, S., Mojaher, Y., Wilkes, G. L., Storey, R. F. and Kennedy, J. P. *Polym. Bull.* 1983, **8**, 281
33 Xu, M., Hu, S., Meiyan, W., Chuanfu, C. and Yongze, J. *Polym. Commun.* 1982, **1**, 27
34 Ivan, B., Kennedy, J. P. and Chang, V. S. C. *J. Polym. Sci.-Chem.* 1980, **18**, 3177
35 Fehervari, A., Kennedy, J. P. and Tudos, F. *J. Macromol. Sci.-Chem.* 1981, **15**, 215
36 Trisler, J. C., Freasier, B. F. and Wu, S. M. *Tetrahedron Lett.* 1974, **42**, 687
37 Chang, V. S. C. and Kennedy, J. P. *Polym. Bull.* 1983, **9**, 479
38 Kratky, O., Pilz, I. and Schmitz, P. J. *J. Colloid Interface Sci.* 1966, **21**, 24
39 Lake, J. A. *Acta. Cryst.* 1967, **23**, 191
40 Schneider, N. S. and Paik Sung, C. S. *Polym. Eng. Sci.* 1977, **17**, 73
41 Seefried, Jr. C. G., Koleske, J. V. and Critchfield, F. E. *J. Appl. Polym. Sci.* 1975, **19**, 2503
42 Zdrahala, R. J., Hager, S. L., Gerkin, R. M. and Critchfield, F. E. *J. Elast. Plast.* 1980, **12**, 225
43 Van Bogart, J. W. C., Gibson, P. E. and Cooper, S. L. *Polymer* 1981, **22**, 1428
44 Brunette, C. M. and MacKnight, W. J. *Rubber Chem. Technol.* 1982, **55**, 1413
45 Froix, M. F. and Pochan, J. M. *J. Polym. Sci.-Phys.* 1976, **14**, 1047
46 Hwang, K. K. S., Speckhard, T. A. and Cooper, S. L., submitted to *J. Macromol. Sci.-Phys.* 1984, **B23**, 153
47 Nielson, L. E. *J. Am. Chem. Soc.* 1953, **75**, 1435
48 Zdrahala, R. J., Critchfield, F. E., Gerkin, R. M. and Hager, S. L. *J. Elast. Plast.* 1980, **12**, 184
49 Seefried, Jr. C. G., Koleske, J. V. and Critchfield, F. E. *J. Appl. Polym. Sci.* 1975, **19**, 2493
50 Saunders, J. H. *Rubber Chem. Tech.* 1960, **33**, 1259
51 Bagrodia, S., Wilkes, G. L., Mohajer, Y., Storey, R. F. and Kennedy, J. P. *Polym. Bull.* 1982, **8**, 281
52 Ruland, W. *J. Appl. Cryst.* 1971, **4**, 70
53 Koberstein, J. T., Morra, B. and Stein, R. S. *J. Appl. Cryst.* 1980, **13**, 34
54 Ruland, W. *Colloid, Polym. Sci.* 1977, **255**, 417

55 Vonk, C. G. *J. Appl. Cryst.* 1973, **6**, 81
56 Porod, G. *Kolloid-Z.* 1951, **124**, 83
57 Koberstein, J. T. and Stein, R. S. *J. Polym. Sci.-Phys.* 1983, **21**, 2181
58 Roe, R. *J. Appl. Cryst.* 1982, **15**, 182
59 Cahn, J. W. and Hilliard, J. E. *J. Chem. Phys.* 1958, **42**, 93
60 Roe, R. J., Fishkis, M. and Chang, J. C. *Macromolecules* 1981, **14**, 1091
61 Neumuller, W. and Bonart, R. *J. Macromol. Sci.-Phys.* 1982, **B21**, 203
62 Bonart, R. and Muller, E. H. *J. Macromol. Sci.-Phys.* 1974, **B10**, 177
63 Bonart, R. and Muller, E. H. *J. Macromol. Sci.-Phys.* 1974, **B10**, 345
64 Van Bogart, J. W. C. *Ph.D. Thesis*, Univ. of Wisconsin, 1981
65 Wood, L. A., Bekkedahl, N. and Roth, F. L. *Ind. Eng. Chem.* 1942, **34**, 1291
66 Kahovec, L., Porod, G. and Ruck, H. *Kolloid Z.-Z. Polym.* 1953, **133**, 16
67 Krause, S. *Macromolecules* 1970, **3**, 84